JOURNAL OF COMPUTATIONAL PHYSICS 23, 23–41 (1977)

A Radial Transport/Fokker–Planck Model for a Tokamak Plasma*

A. A. MIRIN, J. KILLEEN, K. D. MARX, AND M. E. RENSINK

University of California, Lawrence Livermore Laboratory, Livermore, California 94550

Received March 1, 1976; revised May 28, 1976

In neutral-beam heated Tokamaks and the two-energy-component toroidal fusion test reactor (TFTR) there is a warm Maxwellian background plasma which can be described by a set of macroscopic transport equations, and one or more energetic species which are quite non-Maxwellian and should be described by the Fokker–Planck equation. The coupling of these systems is by means of sources of particles and energy in the multispecies transport equations and a time-dependent Maxwellian target plasma in the multispecies Fokker–Planck equations. We have developed a new hybrid code which solves the time-dependent equations of these models simultaneously. Numerical results for a TFTR are presented.

1. INTRODUCTION

In this paper we describe a code to be used for solving the differential equations of plasma transport in toroidal confinement systems. The energetic species are described by velocity space distribution functions, and their slowing down and scattering are modeled numerically by a Fokker–Planck collision operator. The "warm" background ions and electrons are described by a multifluid transport model.

We consider an arbitrary number of such energetic species, which are written as distribution functions in three-dimensional phase space, $f_b(v, \theta, r, t)$, where v is velocity magnitude, θ is the pitch angle and r is the distance from the magnetic axis (see Fig. 1). The poloidal flux is taken to be a function only of r; i.e., surfaces of constant flux are circular tori. We allow for an arbitrary number of background ion species described by densities $n_a(r, t)$, all at the same temperature $T_i(r, t)$. The electrons are described by a separate temperature profile $T_e(r, t)$, and their number density is determined by quasineutrality. Only the poloidal component of the magnetic field, $B_\theta(r, t)$, varies with time.

* Work performed under the auspices of the U. S. Energy Research and Development Administration, Contract W-7405-ENG-48.

ISSN 0021-9991

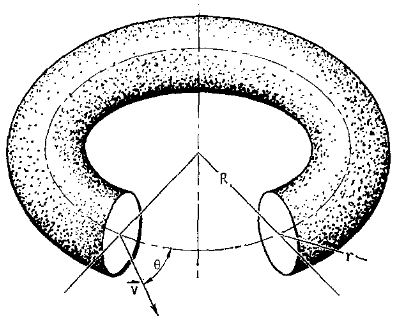

FIG. 1. Coordinate System

2. BASIC EQUATIONS

Our model is described by the equations[1]

$$\partial f_b/\partial t = (\partial f_b/\partial t)_c + H_b - S_{bc} + S_{\alpha b} - c_b f_b + \hat{E}_b\,, \tag{2.1}$$

$$\partial n_a/\partial t = -(1/r)(\partial/\partial r)(r\Gamma_a) + \int (S_{bc} + c_b f_b)\,d\mathbf{v}\cdot\delta(a,b), \tag{2.2}$$

$$(\partial/\partial t)(\tfrac{3}{2}n_e T_e) = -(1/r)(\partial/\partial r)(rQ_e) - Q_\Delta - \hat{Q} + E_z j_z + \sum_b Q_{eb} - \tfrac{3}{2}n_e T_e/\hat{\tau}_e\,, \tag{2.3}$$

$$(\partial/\partial t)\Big(\tfrac{3}{2}\sum_a n_a T_i\Big) = -(1/r)(\partial/\partial r)(rQ_i) + Q_\Delta + \hat{Q} + \sum_{a,b} Q_{ab} + \tfrac{3}{2}T_i\sum_{a,b}\int (S_{bc} + c_b f_b)\,d\mathbf{v}\,\delta(a,b), \tag{2.4}$$

$$\partial B_\theta/\partial t = c(\partial E_z/\partial r). \tag{2.5}$$

Here, H_b is the source profile for species "b"; $S_{\alpha D}$, $S_{\alpha\alpha}$ and $S_{\alpha T}$ are source or loss terms describing the D–T–α reaction; S_{bc} represents the transfer of (low-energy) particles from a hot species to its corresponding background; and $\delta(a, b)$ is the Kronecker delta. The term Γ_a is the particle flux for species "a"; Q_e and Q_i are the electron and ion energy fluxes; Q_Δ and $\hat{Q}$ represent energy transfer between ions and electrons; Q_{ab} represents the heating of species "a" by energetic species "b"; Q_{eb} represents the heating of electrons by energetic species "b"; $E_z j_z$ is ohmic heating; c_b is an inverse charge exchange time; $\hat{E}_b$ describes the acceleration due to the toroidal electric field; and $\hat{\tau}_e$ is the electron energy con-

[1] Throughout the paper summations over plasma species are assumed to include background ions only, except where otherwise noted.

finement time. We write the Fokker–Planck collision operator for the energetic species in conservative form [1]:

$$\frac{1}{{}^*\Gamma_b}\left(\frac{\partial f_b}{\partial t}\right)_c = \frac{1}{v^2}\frac{\partial G_b}{\partial v} + \frac{1}{v^2 \sin\theta}\frac{\partial H_b}{\partial \theta}, \tag{2.6}$$

where

$$G_b = A_b f_b + B_b(\partial f_b/\partial v) + C_b(\partial f_b/\partial \theta) \tag{2.7}$$

and

$$H_b = D_b f_b + E_b(\partial f_b/\partial v) + F_b(\partial f_b/\partial \theta). \tag{2.8}$$

The coefficients of Eqs. (2.7) and (2.8) are given by

$$A_b = \frac{v^2}{2}\frac{\partial^3 g_b}{\partial v^3} + v\frac{\partial^2 g_b}{\partial v^2} - \frac{\partial g_b}{\partial v} - \frac{1}{v}\frac{\partial^2 g_b}{\partial \theta^2} + \frac{1}{2}\frac{\partial^3 g_b}{\partial v\,\partial \theta^2} - \frac{\cot\theta}{v}\frac{\partial g_b}{\partial \theta} + \frac{\cot\theta}{2}\frac{\partial^2 g_b}{\partial v\,\partial\theta} - v^2\frac{\partial h_b}{\partial v}, \tag{2.9}$$

$$B_b = \frac{v^2}{2}\frac{\partial^2 g_b}{\partial v^2}, \tag{2.10}$$

$$C_b = -\frac{1}{2v}\frac{\partial g_b}{\partial \theta} + \frac{1}{2}\frac{\partial^2 g_b}{\partial v\,\partial \theta}, \tag{2.11}$$

$$D_b = \frac{\sin\theta}{2v^2}\frac{\partial^3 g_b}{\partial \theta^3} + \frac{\sin\theta}{2}\frac{\partial^3 g_b}{\partial v^2\,\partial\theta} + \frac{\sin\theta}{v}\frac{\partial^2 g_b}{\partial v\,\partial\theta} - \frac{1}{2v^2\sin\theta}\frac{\partial g_b}{\partial\theta} + \frac{\cos\theta}{2v^2}\frac{\partial^2 g_b}{\partial\theta^2} - \sin\theta\frac{\partial h_b}{\partial\theta}, \tag{2.12}$$

$$E_b = \sin\theta\, C_b, \tag{2.13}$$

$$F_b = \frac{\sin\theta}{2v^2}\frac{\partial^2 g_b}{\partial\theta^2} + \frac{\sin\theta}{2v}\frac{\partial g_b}{\partial v}, \tag{2.14}$$

where

$$\nabla^4 g_b = -8\pi \sum_s \left(\frac{Z_b}{Z_s}\right)^2 \ln \Lambda_{bs} f_s, \tag{2.15}$$

$$\nabla^2 h_b = -4\pi \sum_s \left(\frac{Z_b}{Z_s}\right)^2 \ln \Lambda_{bs}\left(1 + \frac{m_b}{m_s}\right) f_s, \tag{2.16}$$

and

$$\ln \Lambda_{bs} = \ln\left[\left(\frac{m_b m_s}{m_b + m_s}\right)\frac{2\bar{\alpha}\lambda_D}{r_e m_e c}\sup_{k=b,s}\left(\frac{2E_k}{m_k}\right)^{1/2}\right] - \frac{1}{2}. \tag{2.17}$$

Here $\bar{\alpha} = 1/137$ is the fine structure constant, r_e is the classical electron radius $e^2/m_e c^2$, and λ_D is the Debye length. The quantity $*\Gamma_b$ in Eq. (2.6) is given by

$$*\Gamma_b = 4\pi(Z_b e)^4/m_b^2. \tag{2.18}$$

The quantity "s" in Eqs. (2.15) and (2.16) runs over all species; the background ions and electrons are represented as Maxwellians of appropriate density and temperature.

The energy transfer terms Q_{db} of Eqs. (2.3)–(2.4), where "d" = "a" or "e," are defined as

$$Q_{db} = \tfrac{1}{2} m_d \int (\partial f_d/\partial t)_{c,b}\, v^2\, d\mathbf{v}, \tag{2.19}$$

where $(\partial f_d/\partial t)_{c,b}$ represents those terms of Eq. (2.6) involving the Rosenbluth potentials (g_b and h_b) for species "b." Performing the integration in Eq. (2.19), we obtain the formula

$$Q_{db} = (4\pi m_d)(4\pi\ *\Gamma_d \ln \Lambda_{db}(Z_b/Z_d)^2) \int_0^\infty f_d v^2\, dv \cdot \left\{ \int_v^\infty \hat{f}_b x\, dx - (m_d/m_b)(1/v) \int_0^v \hat{f}_b x^2\, dx \right\} \tag{2.20}$$

where

$$\hat{f}_b(v) = \tfrac{1}{2} \int_0^\pi f_b(v, \theta) \sin\theta\, d\theta. \tag{2.21}$$

and f_d is the appropriate Maxwellian.

The particle transfer term S_{bc} of Eq. (2.1) may be defined in two ways. In the first method, we set

$$S_{bc} = (g_b(v, r)/\Delta t) \inf_{v,\theta} (f_b(v, \theta, r)/g_b(v, r)), \tag{2.22}$$

where

$$g_b(v, r) = (m_b/2\pi T_i(r))^{3/2} \exp(-\tfrac{1}{2} m_b v^2/T_i(r)). \tag{2.23}$$

What we are effectively doing here is subtracting an appropriate Maxwellian from the energetic species distribution function, and transferring that number of particles to the corresponding background species. In the second method we set $f_b(v, \theta, r) = 0$ if $\frac{1}{2} m_b v^2 \leqslant \frac{3}{2} T_i(r)$, and compute the number of particles lost across the boundary in velocity space $v = (3T_i(r)/m_b)^{1/2}$. This latter method has the advantage that the resulting energetic distribution functions will tend to be smoother. However, the former method seems more physically correct since a background Maxwellian consists of a sampling of particles of various energies—not a delta function of energy $\frac{3}{2} T_i$; hence, the particle source term should reflect this property. Detailed time dependent comparisons of the two methods have yet to be performed. Preliminary computations indicate, however, that the two methods will most likely compare favorably well.

The toroidal electric field term $\hat{E}_b$ is simply

$$\hat{E}_b = \frac{-Z_b e E_z}{m_b}\left(\cos\theta \frac{\partial f_b}{\partial v} - \frac{\sin\theta}{v}\frac{\partial f_b}{\partial \theta}\right). \tag{2.24}$$

This term has yet to be included in any calculations.

The form of the inverse charge exchange time is

$$c_b = c_{0b}\exp(c_{1b} r/a). \tag{2.25}$$

The fusion terms are given by the expressions

$$S_{\alpha \mathrm{D}} = -n_{\mathrm{T}}\, \overline{\sigma_{\mathrm{DT}} v}\, f_{\mathrm{D}}\,, \tag{2.26}$$

$$S_{\alpha \mathrm{T}} = -n_{\mathrm{D}}\, \overline{\sigma_{\mathrm{DT}} v}\, f_{\mathrm{T}}\,, \tag{2.27}$$

$$S_{\alpha\alpha} = n_{\mathrm{D}} n_{\mathrm{T}}\, \overline{\sigma_{\mathrm{DT}} v} \cdot \delta(v_\alpha - (2(3.5\ \mathrm{MeV}) m_\alpha)^{1/2})/4\pi v^2. \tag{2.28}$$

The primary transport model represents the collisionless (banana) regime. We let

$$\Gamma_a = \Gamma_a{}^c + (n_a/n_e)\,\Gamma_e{}^c, \tag{2.29}$$

$$Q_i = \sum_a (Q_a{}^c + (5/2)(n_a/n_e)\,\Gamma_e{}^c T_i), \tag{2.30}$$

$$Q_e = Q_e{}^c, \tag{2.31}$$

$$Q_\Delta = (3m_e(T_e - T_i)/\tau_e)\sum_a (n_a/m_a)\, Z_a{}^2, \tag{2.32}$$

$$\hat{Q} = e\Gamma_e E_r\,, \tag{2.33}$$

where $\Gamma_a{}^c$, $\Gamma_e{}^c$, $Q_a{}^c$, and $Q_e{}^c$ are Connor's expressions for the fluxes [2], and

$$\Gamma_e = \sum_a Z_a \Gamma_a\,, \tag{2.34}$$

$$\tau_e = 3m_e^{1/2} T_e^{3/2}/4(2\pi)^{1/2}\, e^4 n_e \ln \Lambda_{ee}\,, \tag{2.35}$$

$$E_r = T_i \sum_a \frac{m_a n_a}{Z_a e}\left[\frac{n_a'}{n_a} - 0.17\frac{T_i'}{T_i}\right]\langle\nu_a\rangle \Big/ \sum_a m_a n_a \langle\nu_a\rangle. \tag{2.36}$$

The average collision frequency $\langle\nu\rangle$ is given by

$$\langle\nu_j\rangle = (4/3\pi^{1/2})\int_0^\infty x_j^{3/2} e^{-x_j}\nu_j(x_j)\, dx_j\,, \tag{2.37}$$

where

$$\nu_j = \sum_k \nu_{jk}, \tag{2.38}$$

$$\nu_{jk} = \left(\frac{2^{1/2}\pi e^4 \ln \Lambda_{ee} Z_j^2 Z_k^2 n_k}{m_j^{1/2} T_j^{3/2}}\right) x_j^{-3/2} h\left(\frac{m_k T_j}{m_j T_k} x_j\right), \tag{2.39}$$

$$h(x) = (1 - (1/2x))\,\eta(x) + \eta'(x), \tag{2.40}$$

$$\eta(x) = 2/\pi^{1/2} \int_0^x e^{-t} t^{1/2}\, dt. \tag{2.41}$$

Here, "j" and "k" stand for either "a" or "e" (plasma ions or electrons). Eqs. (2.29) and (2.30) basically agree with Connor's expressions since for a multi-ion plasma $\Gamma_e^c \ll \Gamma_a^c$; however, it is necessary to add the correction terms proportional to Γ_e^c so that the model consistently represents both simple and multispecies plasmas.[2] The expression for the toroidal electric field E_z is given by

$$E_z = (m_e/n_e e^2 \tau_e \delta_4)(1 + \delta_5 (r/R)^{1/2})^{-1} j_e, \tag{2.42}$$

where

$$j_z = j_e + j_g = (c/4\pi)(1/r)(\partial/\partial r)(rB_\theta) \tag{2.43}$$

and j_g is the bootstrap current, for which a formula is given in Appendix A. The expression for j_g has not been properly generalized for multispecies plasmas due to its high degree of complexity. The values of δ_4 and δ_5 in Eq. (2.42) are defined in Appendix A.

It is convenient to write the transport model in a more general form so that the form of the transport coeficients can be changed without modifying the basic structure of the code. We let

$$\Gamma_a = \sum_b D_{ab}^d(\partial n_b/\partial r) + D_a^i(\partial T_i/\partial r) + D_a^e(\partial T_e/\partial r) + D_a^z E_z, \tag{2.44}$$

$$Q_i = \sum_b L_b^d(\partial n_b/\partial r) + L^i(\partial T_i/\partial r) + L^e(\partial T_e^e/\partial r) + L^z E_z, \tag{2.45}$$

$$Q_e = \sum_b M_b^d(\partial n_b/\partial r) + M^i(\partial T_i/\partial r) + M^e(\partial T_e/\partial r) + M^z E_z, \tag{2.46}$$

$$E_z = \sum_b K_b^d(\partial n_b/\partial r) + K^i(\partial T_i/\partial r) + K^e(\partial T_e/\partial r) + K^z(1/r)(\partial/\partial r)(rB_\theta), \tag{2.47}$$

$$\hat{Q} = \left[\sum_b R_b^d(\partial n_b/\partial r) + R^i(\partial T_i/\partial r)\right] \sum_b Z_b \Gamma_b, \tag{2.48}$$

$$Q_\Delta = \sum_b \hat{\nu}_b n_b (T_e - T_i). \tag{2.49}$$

Expressions for the coefficients in Eqs. (2.44)–(2.49) are given in Appendix A.

[2] For a simple plasma $\Gamma_a^c = 0$, and Γ_a should equal Γ_e^c/Z_a.

In addition to the "banana" regime, the "smoothed banana-plateau" regime of Hinton *et al.* [3] may be implemented. Approximations for these coefficients derived by Rutherford [4] appear in Appendix B.

3. Numerical Techniques

The Fokker–Planck collision operator, Eq. (2.6), is integrated using a split semi-implicit difference algorithm:

$$(f_b^1 - f_b^0)/\Delta t = ({}^*\Gamma_b/v_j^2)(\partial G_b/\partial v)_{i,j} \tag{3.1}$$

$$(f_b^2 - f_b^1)/\Delta t = ({}^*\Gamma_b/v_j^2 \sin\theta_i)(\partial H_b/\partial\theta)_{i,j} \tag{3.2}$$

$$\begin{aligned}\left(\frac{\partial G_b}{\partial v}\right)_{i,j} = {} & \frac{A^0_{i,j+1} f^1_{i,j+1} - A^0_{i,j-1} f^1_{i,j-1}}{2\Delta v_j} \\ & + \frac{1}{\Delta v_j}\left[\frac{B^0_{i,j+1/2}(f^1_{i,j+1} - f^1_{i,j})}{\Delta v_{j+1/2}} - \frac{B^0_{i,j-1/2}(f^1_{i,j} - f^1_{i,j-1})}{\Delta v_{j-1/2}}\right] \\ & + \frac{1}{2\Delta v_j}\left[\frac{C^0_{i,j+1}(f^0_{i+1,j+1} - f^0_{i-1,j+1})}{2\Delta\theta_i} - \frac{C^0_{i,j-1}(f^0_{i+1,j-1} - f^0_{i-1,j-1})}{2\Delta\theta_i}\right],\end{aligned} \tag{3.3}$$

$$\begin{aligned}\left(\frac{\partial H_b}{\partial \theta}\right)_{i,j} = {} & \frac{D^0_{i+1,j} f^2_{i+1,j} - D^0_{i-1,j} f^2_{i-1,j}}{2\Delta\theta_i} \\ & + \frac{1}{2\Delta\theta_i}\left[\frac{E^0_{i+1,j}(f^1_{i+1,j+1} - f^1_{i+1,j-1})}{2\Delta v_j} - \frac{E^0_{i-1,j}(f^1_{i-1,j+1} - f^1_{i-1,j-1})}{2\Delta v_j}\right] \\ & + \frac{1}{\Delta\theta_i}\left[\frac{F^0_{i+1/2,j}(f^2_{i+1,j} - f^2_{i,j})}{\Delta\theta_{i+1/2}} - \frac{F^0_{i-1/2,j}(f^2_{i,j} - f^2_{i-1,j})}{\Delta\theta_{i-1/2}}\right],\end{aligned} \tag{3.4}$$

where $f_{ij} = f(v_j, \theta_i)$, and the subscript "$b$" has been dropped. The superscript "0" represents the data at time-step n, "1" represents the intermediate data, and "2" refers to the data at time-step $n + 1$. Also,

$$B_{i,j\pm 1/2} = \tfrac{1}{2}(B_{i,j} + B_{i,j\pm 1}) \tag{3.5}$$

$$F_{i\pm 1/2,j} = \tfrac{1}{2}(F_{i,j} + F_{i\pm 1,j}) \tag{3.6}$$

$$\Delta v_{j\pm 1/2} = \pm(v_{j\pm 1} - v_j) \tag{3.7}$$

$$\Delta\theta_{i\pm 1/2} = \pm(\theta_{i\pm 1} - \theta_i) \tag{3.8}$$

$$\Delta v_j = \tfrac{1}{2}(\Delta v_{j+1/2} + \Delta v_{j-1/2}) \tag{3.9}$$

$$\Delta\theta_i = \tfrac{1}{2}(\Delta\theta_{i+1/2} + \Delta\theta_{i-1/2}). \tag{3.10}$$

We see that Eq. (2.6) is differenced in conservative form; that is, the density of particles will be precisely conserved modulo boundary terms. One drawback, however, is that the method is only first-order accurate for a general nonuniform mesh. Note also that the terms of mixed derivative type are treated explicitly. This is done so that the difference equations may be expressed in tridiagonal form.

Eqs. (2.2)–(2.5) are differenced using a semi-implicit iterative technique. We may express Eqs. (2.2)–(2.5) in vector form as

$$\mathbf{A}(\partial \mathbf{U}/\partial t) = \mathscr{L}(\mathbf{U}) \tag{3.11}$$

where $\mathbf{U}$ is a $K + 3$ component vector consisting of K densities, the ion and electron energies and the poloidal magnetic field, and the matrix $\mathbf{A}$ accounts for the fact the $K + 1$ and $K + 2$ components of the vector $(\partial \mathbf{U}/\partial t)$ differ from the respective terms on the left hand sides of Eqs. (2.3)–(2.4). We write

$$(\mathbf{U}_l^{n+1} - \mathbf{U}_l^{n})/\Delta t = \mathbf{A}^{-1}[\rho \mathscr{L}^*(\mathbf{U}^{n+1}) + (1 - \rho)\, \mathscr{L}(\mathbf{U}^n)] \tag{3.12}$$

where the implicit operator $\mathscr{L}^*$ is linearized with coefficients depending on the latest iterate. Products of implicit derivatives are written as

$$((\partial f/\partial r)(\partial g/\partial r))^{n+1} = (1/2)[(\partial f/\partial r)^{n+1}(\partial g/\partial r)^* + (\partial f/\partial r)^*(\partial g/\partial r)^{n+1}] \tag{3.13}$$

where $*$ refers to the latest iterate. Derivatives of the form $(1/r)(\partial/\partial r)(D(\partial h/\partial r))$ are approximated as

$$\frac{1}{r}\frac{\partial}{\partial r}\left(D\frac{\partial h}{\partial r}\right) = \frac{1}{r_l\,\Delta r_l}\left[D_{l+1/2}\left(\frac{h_{l+1} - h_l}{\Delta r_{l+1/2}}\right) - D_{l-1/2}\left(\frac{h_l - h_{l-1}}{\Delta r_{l-1/2}}\right)\right]. \tag{3.14}$$

Eq. (3.12) is, in general, only first order accurate in space, but both density and energy density will be conserved. All of the spatial differences involve at most 3 points, so that Eq. (3.12) may be viewed as a vector tridiagonal system. A method for solving such systems is presented by Killeen *et al.* [1].

It should be noted that the Fokker–Planck equations for the energetic species need not be computed at each radial meshpoint. Our model contains an option whereby the energetic distributions are stored and advanced at every Kth value of r, with K arbitrary. Relevant quantities at intermediate radial points (e.g., energy transfer) may then be computed using some form of interpolation—at this writing, either linear or cubic splines. This option is indispensable for the efficient running of the code, for most of the computer time is spent integrating the Fokker–Planck equations.

4. Boundary Conditions

The boundary conditions for the distribution function $f_b(v, \theta, r)$ are:

$$f_b(\infty, \theta, r) = 0 \tag{4.1}$$

$$(\partial f_b/\partial v)(0, \pi/2, r) = 0 \tag{4.2}$$

$$(\partial/\partial\theta) f_b(0, \theta, r) = 0 \tag{4.3}$$

$$(\partial f_b/\partial\theta)(v, 0, r) = (\partial f_b/\partial\theta)(v, \pi, r) = 0. \tag{4.4}$$

In an attempt to impose density conservation, Eqs. (4.2)–(4.4) are replaced by conservation conditions of the form

$$(\partial/\partial v)(A_b f_b + B_b(\partial f_b/\partial v)) = 0 \tag{4.5}$$

and

$$(\partial/\partial\theta)(D_b f_b + F_b(\partial f_b/\partial\theta)) = 0. \tag{4.6}$$

These equations are evaluated one half mesh-point from the respective boundaries.

The boundary conditions for the "transport" dependent variables are:

$$(\partial n_a/\partial r)(r = 0) = 0 \tag{4.7}$$

$$(\partial T_e/\partial r)(r = 0) = 0 \tag{4.8}$$

$$(\partial T_i/\partial r)(r = 0) = 0 \tag{4.9}$$

$$B_\theta(r = 0) = 0 \tag{4.10}$$

$$n_a(r = 0) = \psi_a(t) \tag{4.11}$$

$$T_e(r = a) = \psi_e(t) \tag{4.12}$$

$$T_i(r = a) = \psi_i(t) \tag{4.13}$$

$$(\partial B_\theta/\partial t)(r = a) = 0. \tag{4.14}$$

Eqs. (4.7)–(4.9) are also replaced by conservation boundary conditions in an attempt to impose density and energy-density conservation.

5. Diagnostics

We compute the total particle number and energy for each species[3]

$$N_p = (2\pi)^2 R \int_0^a n_p(r)\, r\, dr \tag{5.1}$$

$$N_p\langle T_p\rangle = (2\pi)^2 R \int_0^a n_p(r)\, T_p(r)\, r\, dr. \tag{5.2}$$

[3] All energy integrals computed here are $\frac{2}{3}$ of the true energy.

Here R is the major radius, a is the minor radius, and for the energetic species $T_p(r)$ is two-thirds of the mean energy per particle. We also keep track of the number of injected particles and the injected energy.

$$N_b^i = (2\pi)^2 R \int_0^t \int_0^a J_b(r, t)\, r\, dr\, dt \tag{5.3}$$

$$N_b^i \langle T_b^i \rangle = (2\pi)^2 R \int_0^t \int_0^a J_b(r, t)\, T_b^i(r, t)\, r\, dr\, dt \tag{5.4}$$

$$N_b^e = N_b^i \tag{5.5}$$

$$N_b^e \langle T_b^e \rangle = (2\pi)^2 R \int_0^t \int_0^a J_b(r, t)\, Z_b T_e^i(r, t)\, r\, dr\, dt. \tag{5.6}$$

Here $T_b^i(r)$ is the species "b" source temperature profile, $T_e^i(r)$ is the corresponding electron source temperature profile, and $J_b(r)$ is the appropriate source current.

The number of particles and total energy lost at the limiter are equal to

$$N_a^{\text{lim}} = (2\pi)^2 R \int_0^t \Gamma_a(r = a, t)\, dt \tag{5.7}$$

$$\sum_a N_a^{\text{lim}} \langle T_i^{\text{lim}} \rangle = (2\pi)^2 R \cdot \tfrac{2}{3} \int_0^t Q_i(r = a, t)\, dt \tag{5.8}$$

$$N_e^{\text{lim}} \langle T_e^{\text{lim}} \rangle = (2\pi)^2 R \cdot \tfrac{2}{3} \int_0^t Q_e(r = a, t)\, dt. \tag{5.9}$$

The ohmic heating input energy is

$$Q_e = (2\pi)^2 R \int_0^t \int_0^a j_z(r, t)\, E_z(r, t)\, r\, dr\, dt \tag{5.10}$$

and the fusion energy is equal to

$$F_e = (2\pi)^2 R \int_0^t \int_0^a n_{\text{D}}(r, t)\, n_{\text{T}}(r, t)\, \overline{\sigma_{\text{DT}} v}\, E_f r\, dr\, dt \tag{5.11}$$

where $E_f = 17.6$ MeV and σ_{DT} is the D–T–α reaction cross-section. The approximation used for σ_{DT} is given by Futch *et al.* [5], and the computation of $\overline{\sigma_{\text{DT}} v}$ is discussed in Marx *et al.* [6].

6. Numerical Results

We first present a one-ion (protons) transport-only problem in which the toroidal minor radius a is 14 cm, the major radius R is 109 cm, and the toroidal magnetic field B_ϕ is 30 kG. The total current I, given by

$$I = 2\pi \int_0^a j_z(r)\, r\, dr \tag{6.1}$$

is 40 kA, and the current density is of the form

$$j_z(r) \sim (1 - r^2/a^2). \tag{6.2}$$

The initial density and temperature profiles are

$$n(r) = 10^{13}[1 - .8(r/a)^2]\ \mathrm{cm}^{-3} \tag{6.3}$$

$$T_e(r) = .2[1 - .8(r/a)^2]\ \mathrm{keV} \tag{6.4}$$

$$T_i(r) = .02\ \mathrm{keV} \tag{6.5}$$

and the limiter values ($r = a$) are held constant in time.

This problem was run for a total of 60 msec at a time step of 0.1 msec, using the smoothed banana-plateau coefficients of Appendix B. Figures 2–5 contain profiles of the density, electron temperature, ion temperature and toroidal current density, respectively. The temperatures have risen substantially since $t = 0$. There is a mild depression of the density profile and humps in the T_e and j_z profiles near the "limiter" $r = a$; these are known as "skin effects" (referring to the skin of the torus), and the do not occur to any real extent experimentally.

These results basically agree with those of Hinton *et al.* [8], except for the fact that the on-axis T_e and T_i values are off by about 10%. This is attributable to

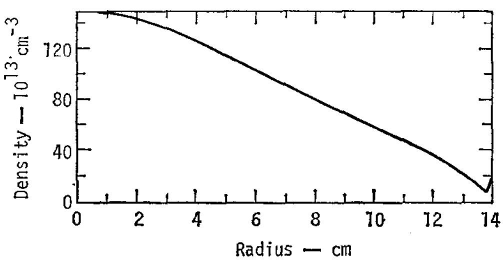

FIG. 2. $n(r)$ (part/cm^3) at $t = 60$ ms (transport-only prob.).

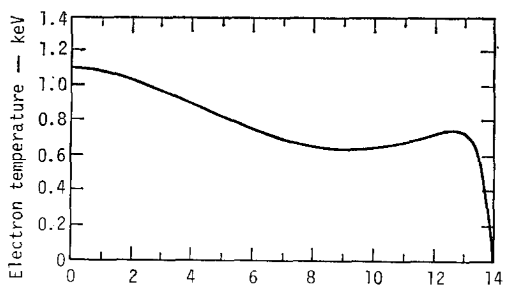

FIG. 3. $T_e(r)$ (kev) at $t = 60$ ms (transport-only prob.).

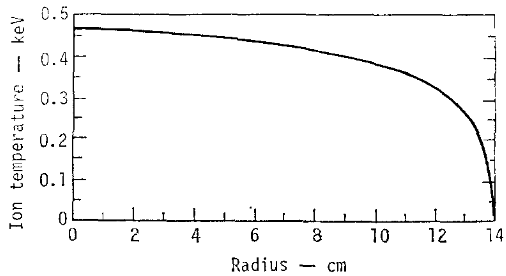

FIG. 4. $T_i(r)$ (kev) at $t = 60$ ms (transport-only prob.).

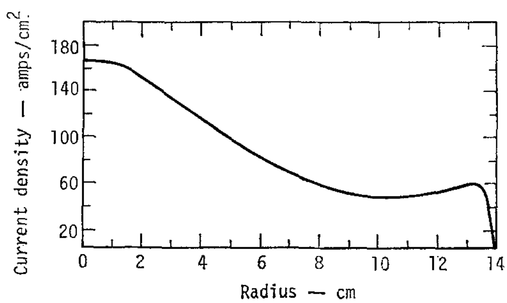

FIG. 5. $j_z(r)$ (amps/cm²) at $t = 60$ ms (transport-only prob.).

differences in our respective transport models, some of which are noted in Appendix A.

We now present a D–T Fokker–Planck transport problem in which $a = 90$ cm, $R = 270$ cm, $B_\phi = 45$ kG and $I = 2.5$ MA. There is initially a background tritium plasma satisfying

$$n_T(r) = 2 \times 10^{14}[1 - .8(r/a)^2]\ \text{cm}^{-3}, \tag{6.6}$$

$$T_i(r) = 8[1 - \tfrac{15}{16}(r/a)^2]\ \text{keV}, \tag{6.7}$$

$$T_e(r) = T_i(r), \tag{6.8}$$

and the initial current profile is given by Eq. (6.2). We inject a deuterium beam of 120 keV from $t = 10$ msec to $t = 300$ msec and calculate up to $t = 2000$ msec at a time-step of 2.0 msec. The beam current density is

$$J_b(r) = 8.11 \times 10^{13}(.9e^{-4(r/a)^2}) \tag{6.9}$$

and the total current is 180 amps. The quantities $T_e(a)$, $T_i(a)$ and $n_T(a)$ are held constant in time, but $n_D(a)$ is allowed to increase in time to take account of the transfer of energetic particles to the background plasma. The transport regime is the banana regime of Appendix A.

Figure 6 contains a plot of the fusion energy generated and the injected beam energy as functions of time. The "beam generated fusion energy" is that component

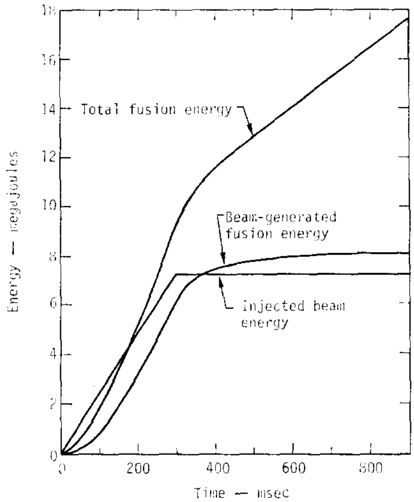

FIG. 6. Fusion energy vs. time (F.P. transport prob.).

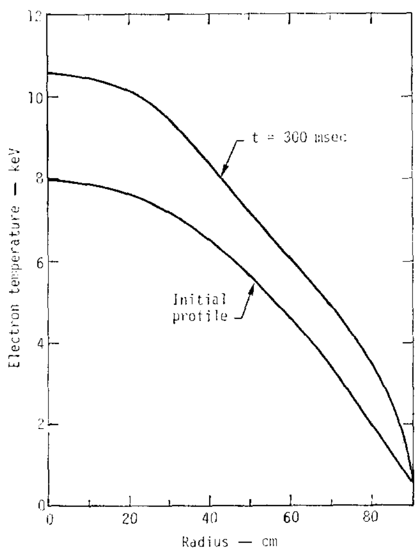

FIG. 7. $T_e(r)$ at $t = 0$ and 300 ms (F.P. transport prob.).

of fusion energy which remains after the steady state component is subtracted out; i.e., we subtract from Eq. (5.11) a term of the form "ct," where c is the steady state fusion reaction rate. We see that the figure of merit Q, defined as the net fusion energy divided by the injected energy, is greater than 1. Figure 7 shows the profile $T_e(r)$ at $t = 0$ and $t = 300$ msec. We see that the electrons have heated up due to the presence of the hot deuterium. Figure 8 shows the deuterium density as a function of r at $t = 300$ and $t = 2000$ msec. We see that diffusion has taken place in that time period. Lastly, Fig. 9 shows a three-dimensional plot of the hot deuterium distribution function at $r = 67.5$ cm, $t = 200$ msec.

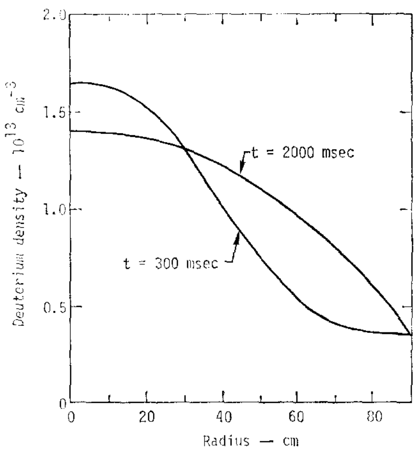

FIG. 8. $n_D(r)$ at $t = 300$ and 2000 ms (F.P. transport prob.).

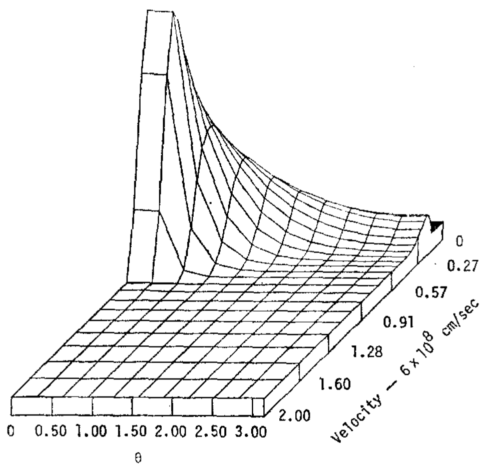

FIG. 9. $f_b(v, \theta, r = 67.5$ cm, $t = 200$ ms) (F.P. transport prob.).

7. Future Plans

Future plans call for making the following improvements:

(A) The model will be generalized to allow for noncircular flux surfaces.

(B) Particle orbit loss regions will be inserted into velocity space.

(C) Magnetic compression will be added.

(D) A more detailed description of neutrals will be added.

(E) The transport coefficients will be upgraded.

(F) A more detailed description of beam deposition will be added.

(G) The condition that the background ions all be at the same temperature will be relaxed.

Appendix A

The coefficients of Eqs. (2.44)–(2.49) for the "banana" regime are:

$$D_{ab}^{d} = \frac{-1.48c^2(r/R)^{1/2}}{e^2 B_\theta^{2}} \cdot \frac{1}{\sum_s m_s n_s \langle \nu_s \rangle} \Bigg[\frac{m_a n_a \langle \nu_a \rangle}{Z_a} \cdot \left\{ \sum_s m_s n_s \langle \nu_s \rangle \frac{T_i \delta_{ab}}{Z_a n_a} - \frac{m_b \langle \nu_b \rangle T_i}{Z_b} \right\} + m_e n_a \langle \nu_e \rangle \left\{ \sum_s m_s n_s \langle \nu_s \rangle \frac{T_e Z_b}{n_e} + m_b \langle \nu_b \rangle \frac{T_i}{Z_b} \right\} \Bigg], \tag{A.1}$$

$$D_a^{i} = \frac{1.48c^2(r/R)^{1/2}}{e^2 B_\theta^{2}} \cdot \frac{1}{\sum_s m_s n_s \langle \nu_s \rangle} \Bigg[\frac{m_a n_a \langle \nu_a \rangle}{Z_a} \cdot \left\{ \sum_s m_s n_s \langle \nu_s \rangle \left(\frac{1}{Z_a} \left(\frac{3}{2} - \frac{\langle x_a \nu_a \rangle}{\langle \nu_a \rangle} \right) - \frac{1}{Z_s} \left(\frac{3}{2} - \frac{\langle x_s \nu_s \rangle}{\langle \nu_s \rangle} \right) \right) \right] + m_e n_a \langle \nu_e \rangle \sum_s \frac{m_s n_s \langle \nu_s \rangle}{Z_s} \left(\frac{3}{2} - \frac{\langle x_s \nu_s \rangle}{\langle \nu_s \rangle} \right) \Bigg], \tag{A.2}$$

$$D_a^{e} = \frac{1.48c^2(r/R)^{1/2}}{e^2 B_\theta^{2}} m_e n_a \langle \nu_e \rangle \left(\frac{3}{2} - \frac{\langle x_e \nu_e \rangle}{\langle \nu_e \rangle} \right), \tag{A.3}$$

$$D_a^{z} = -\,1.48c \left(\frac{r}{R} \right)^{1/2} \frac{n_a}{B_\theta} \left\{ 1 + \frac{\langle \nu_{ee} \rangle \langle \nu_{ee}/\nu_e \rangle}{\langle \nu_{ee}(\nu_e - \nu_{ee})/\nu_e \rangle} \right\}, \tag{A.4}$$

$$L_b{}^d = \frac{-1.48c^2(r/R)^{1/2}\, T_i}{e^2 B_\theta{}^2 \sum_s m_s n_s \langle \nu_s \rangle} \Bigg[\frac{m_b T_i}{Z_b} \cdot \left(\frac{\langle x_b \nu_b \rangle}{Z_b} \sum_s m_s n_s \langle \nu_s \rangle - \langle \nu_b \rangle \sum_s \frac{m_s n_s \langle x_s \nu_s \rangle}{Z_s} \right) + \frac{5}{2} m_e \langle \nu_e \rangle \sum_c n_c \cdot \left(\sum_s m_s n_s \langle \nu_s \rangle \frac{T_e Z_b}{n_e} + m_b \langle \nu_b \rangle\, T_i / Z_b \right) \Bigg], \tag{A.5}$$

$$L^i = \frac{1.48c^2(r/R)^{1/2}\, T_i}{e^2 B_\theta{}^2 \sum_s m_s n_s \langle \nu_s \rangle} \Bigg[\sum_{c,s} \frac{m_c m_s n_c n_s \langle \nu_s \rangle \langle x_c \nu_c \rangle}{Z_c} \cdot \left(\frac{1}{Z_c} \left(\frac{3}{2} - \frac{\langle x_c \nu_c \rangle}{\langle \nu_c \rangle} \right) - \frac{1}{Z_s} \left(\frac{3}{2} - \frac{\langle x_s \nu_s \rangle}{\langle \nu_s \rangle} \right) \right) + \frac{5}{2} m_e \sum_c n_c \langle \nu_e \rangle \sum_s \frac{m_s n_s \langle \nu_s \rangle}{Z_s} \left(\frac{3}{2} - \frac{\langle x_s \nu_s \rangle}{\langle \nu_s \rangle} \right) - \sum_s m_s n_s \langle \nu_s \rangle \sum_c \frac{m_c n_c \langle x_c \nu_c \rangle}{Z_c^2} \left[\frac{\langle x_c{}^2 \nu_c \rangle}{\langle x_c \nu_c \rangle} - \frac{\langle x_c \nu_c \rangle}{\langle \nu_c \rangle} \right] \Bigg], \tag{A.6}$$

$$L^e = \frac{3.7c^2(r/R)^{1/2}\, T_i}{e^2 B_\theta{}^2} m_e \sum_c n_c \langle \nu_e \rangle \left(\frac{3}{2} - \frac{\langle x_e \nu_e \rangle}{\langle \nu_e \rangle} \right), \tag{A.7}$$

$$L^z = \frac{-3.7c(r/R)^{1/2}}{B_\theta} \sum_c n_c T_i \left[1 + \frac{\langle \nu_{ee} \rangle \langle \nu_{ee}/\nu_e \rangle}{\langle \nu_{ee}(\nu_e - \nu_{ee})/\nu_e \rangle} \right], \tag{A.8}$$

$$M_b{}^d = \frac{-1.48c^2(r/R)^{1/2}}{e^2 B_\theta{}^2}\, T_e m_e n_e \langle x_e \nu_e \rangle \left(\frac{T_e Z_b}{n_e} + \frac{T_i m_b \langle \nu_b \rangle}{Z_b \sum_s m_s n_s \langle \nu_s \rangle} \right), \tag{A.9}$$

$$M^i = \frac{1.48c^2(r/R)^{1/2}}{e^2 B_\theta{}^2} \frac{T_e m_e n_e \langle x_e \nu_e \rangle}{\sum_s m_s n_s \langle \nu_s \rangle} \left(\sum_s \frac{m_s n_s \langle \nu_s \rangle}{Z_s} \left(\frac{3}{2} - \frac{\langle x_s \nu_s \rangle}{\langle \nu_s \rangle} \right) \right), \tag{A.10}$$

$$M^e = \frac{1.48c^2(r/R)^{1/2}}{e^2 B_\theta{}^2}\, T_e m_e n_e \langle x_e \nu_e \rangle \left(\frac{3}{2} - \frac{\langle x_e{}^2 \nu_e \rangle}{\langle x_e \nu_e \rangle} \right), \tag{A.11}$$

$$M^z = \frac{-1.48c(r/R)^{1/2}\, n_e T_e}{B_\theta} \left[\frac{5}{2} + \frac{\langle x_e \nu_{ee} \rangle \langle \nu_{ee}/\nu_e \rangle}{\langle \nu_{ee}(\nu_e - \nu_{ee})/\nu_e \rangle} \right], \tag{A.12}$$

$$K_b{}^d = (-m_e/\delta_4 e^2 n_e \tau_e)(1 + \delta_5 (r/R)^{1/2})^{-1}\, (c/B_\theta)(r/R)^{1/2}\, \delta_1 (T_e + T_i), \tag{A.13}$$

$$K^i = (-m_e/\delta_4 e^2 \tau_e)(1 + \delta_5 (r/R)^{1/2})^{-1}\, (c/B_\theta)(r/R)^{1/2}\, \delta_3\,, \tag{A.14}$$

$$K^e = (\delta_2/\delta_3)\, K^i, \tag{A.15}$$

$$K^z = (m_e/\delta_4 e^2 n_e \tau_e)(1 + \delta_5 (r/R)^{1/2})^{-1} (c/4\pi), \tag{A.16}$$

$$R_b{}^d = \left(T_i m_b \langle \nu_b \rangle \Big/ Z_b \sum_s m_s n_s \langle \nu_s \rangle\right), \tag{A.17}$$

$$R^i = -.17 \sum_s m_s n_s \langle \nu_s \rangle / Z_s \Big/ \sum_s m_s n_s \langle \nu_s \rangle, \tag{A.18}$$

$$\hat{\nu}_b = (3m_e/\tau_e)(Z_b{}^2/m_b), \tag{A.19}$$

where

$$\delta_4 = K_1(Z_{\text{eff}}), \tag{A.20}$$

$$\delta_5 = -1.48(1 + \tau_e \langle \nu_{ee} \rangle\, K_0{}^2(Z_{\text{eff}})/K_1(Z_{\text{eff}})), \tag{A.21}$$

$$Z_{\text{eff}} = \sum_a n_a Z_a{}^2/n_e\,, \tag{A.22}$$

$$K_0(\beta) = \langle \nu_{ee}/\nu_e \rangle / \tau_e \langle \nu_{ee}(\nu_e - \nu_{ee})/\nu_e \rangle, \tag{A.23}$$

$$K_1(\beta) = \tau_e^{-1} [\langle \nu_e^{-1} \rangle + (\langle \nu_{ee}/\nu_e \rangle^2 / \langle \nu_{ee}(\nu_e - \nu_{ee})/\nu_e \rangle)]. \tag{A.24}$$

The values of δ_4 and δ_5 disagree with those of Hinton *et al.* [8] and Rosenbluth *et al.* [7] because of imperfections in the treatment of nonlocalized distribution functions by Connor's [2] model collision operator.

Since $\delta_5 < 0$, there will be a singularity in Eqs. (A.13)–(A.16) if the aspect ratio R/a is less than $\delta_5{}^2$. In such a case, the correction term $\delta_5(r/R)^{1/2}$ makes little sense, so it is ignored.

The bootstrap current j_g is defined by

$$j_g = \frac{c}{B_\theta}\left(\frac{r}{R}\right)^{1/2} n_e \left\{\sum_a \delta_1 (T_e + T_i) \frac{1}{n_e}\frac{\partial n_a}{\partial r} + \delta_2 \frac{\partial T_e}{\partial r} + \delta_3 \frac{\partial T_i}{\partial r}\right\}, \tag{A.25}$$

where $\delta_1 = -2.44$, $\delta_2 = -0.96$ and $\delta_3 = 0.42$.

Appendix B

The coefficients in Eqs. (2.42)–(2.49) for the "smoothed banana-plateau" regime may be written in the following form:

$$C_{\text{SBP}} = C_{\text{B}} f(C) \tag{B.1}$$

where C_{B} is the coefficient C for the banana regime, as defined in Appendix A, and C_{SBP} is the value for the smoothed banana-plateau regime.

Values of the various $f(C)$ may be found in Table B–1.

TABLE B–1

C		$f(C)$
D^d_{ab}		α_1/α_1^0
D_a^i		α_3/α_3^0
D_a^e		α_2/α_2^0
D_a^z		α_4/α_4^0
M_b^d		β_1/β_1^0
M^i		β_3/β_3^0
M^e		β_2/β_2^0
M^z		β_4/β_4^0
L_b^d	$\frac{5}{2}\Gamma T_i$ terms	$\alpha_1/\alpha_1^0 \cdot y/1.33$
	other terms	γ_3/γ_3^0
L^i	$\frac{5}{2}\Gamma T_i$ terms	$\alpha_3/\alpha_3^0 \cdot y/1.33$
	other terms	γ_3/γ_3^0
L^e		$\alpha_2/\alpha_2^0 \cdot y/1.33$
L^z		$\alpha_4/\alpha_4^0 \cdot y/1.33$
R^i		$(1.5 - y)/.17$
δ_k	$(k = 1,..., 5)$	δ_k^1/δ_k^0

Here,

$$\alpha_1 = -1.12/(1. + 1.78\nu_e^*) \tag{B.2}$$
$$\alpha_2 = -1.5\alpha_1 - 1.25/(1. + .66\nu_e^*) \tag{B.3}$$
$$\alpha_3 = (y - 1.5)\,\alpha_1 \tag{B.4}$$
$$\alpha_4 = -2.44/(1. + .85\nu_e^*) \tag{B.5}$$
$$\beta_1 = -1.25/(1. + .66\nu_e^*) \tag{B.6}$$
$$\beta_2 = -1.5\beta_1 - 2.64/(1. + .35\nu_e^*) \tag{B.7}$$
$$\beta_3 = (y - 1.5)\,\beta_1 \tag{B.8}$$
$$\beta_4 = -4.35/(1. + .4\nu_e^*) \tag{B.9}$$
$$\gamma_3 = -0.48/(1. + .36\nu_i^*) \tag{B.10}$$
$$\delta_1^1 = \alpha_4 \tag{B.11}$$
$$\delta_2^1 = -1.5\delta_1^1 + \beta_4 \tag{B.12}$$
$$\delta_3^1 = (y - 1.5)\,\delta_1^1 \tag{B.13}$$
$$\delta_4^1 = 1.96 \tag{B.14}$$
$$\delta_5^1 = -1.96/(1. + \nu_e^*) \tag{B.15}$$
$$\nu_i^* = 4\,\sqrt{\pi}\,R^{3/2}B_\phi n_e e^4 \ln \Lambda_{ee}/3r^{1/2}B_\theta T_i^2 \tag{B.16}$$
$$\nu_e^* = \sqrt{2}\,T_i^2\nu_i^*/T_e^2 \tag{B.17}$$
$$y = (1.33 + 3\nu_i^*)/(1 + \nu_i^*). \tag{B.18}$$

The superscript "0" in Table B–1 means that the superscripted variable should be evaluated with $\nu_e{}^* = \nu_i{}^* = 0$.

References

1. J. Killeen, A. A. Mirin, and M. E. Rensink, Methods Comput. Phys. **16** (1975), Chap. 11.
2. J. W. Connor, *Plasma Phys.* **15** (1973), 765–782.
3. F. L. Hinton and M. N. Rosenbluth, *Phys. Fluids* **16** (1973), 836–854.
4. P. H. Rutherford, private communication, 7 February 1972.
5. A. H. Futch, Jr., J. P. Holdren, J. Killeen, and A. A. Mirin, *Plasma Phys.* **14** (1972), 211–244.
6. K. D. Marx, A. A. Mirin, M. G. McCoy, M. E. Rensink, and J. Killeen, Calculation of $(\overline{\sigma v})_{\mathrm{DT}}$ for anisotropic mirror and toroidal distributions, to appear.
7. M. N. Rosenbluth, R. D. Hazeltine, and F. L. Hinton, *Phys. Fluids* **15** (1972), 116–140.
8. F. L. Hinton, J. C. Wiley, D. F. Düchs, H. P. Furth, and P. H. Rutherford, *Phys. Rev. Lett.* **29** (1972), 698–701.